Presented at the 31st European PV Solar Energy Conference and Exhibition, 14-18 September 2015, Hamburg, Germany

DEVELOPMENT OF MULTICRYSTALLINE SILICON FOR 20 % EFFICIENT N-TYPE SOLAR CELLS

Stephan Riepe, Patricia Krenckel, Florian Schindler, Claudia Schmid,
Theresa Strauch, Jan Benick, Martin C. Schubert
Fraunhofer Institute for Solar Energy Systems
Heidenhofstrasse 2, D-79110 Freiburg, Germany
Phone: +49 761 4588 5636, Fax: +49 761 4588 9250
E-mail: Stephan.Riepe@ise.fraunhofer.de

ABSTRACT: Multicrystalline silicon suitable for high efficient n-type solar cells has been developed by directional solidification with seeded growth. The effect of varying initial grain sizes on mean grain size and dislocated area fraction over ingot height has been studied by applying different seeding compositions. Granular seed material resulted in the smallest initial grain size at the ingot bottom and the lowest dislocated area fraction at each ingot height. Lifetime analysis before and after a Boron diffusion step revealed that recombination in dislocated areas as well as grain boundaries can limit the mean lifetime in different heights in the same ingot. The efficiencies of solar cells with the TOPCon structure on these materials were predicted by an ELBA analysis. By use of a multicrystalline silicon plate as seed material a high quality material with a predicted cell efficiency of 20 % for processed isotextured wafers of the top ingot region could be realised. Solar cell efficiencies exceeding 21 % are expected if further material optimization by suitable seed selection and an adapted texturing process is applied.

Keywords: Crystallisation, Multicrystalline Silicon, n-type

1 INTRODUCTION

The quality of multicrystalline silicon (mc-Si) material for solar cells has made significant progress by the development of ingots with strongly reduced amount of dislocations. This type of material is now mostly referred to as "High Performance Multicrystalline Silicon" (HPM-Si) [1]. Due to performance advantages over standard mc-Si, this material is expected to have a high market share in the near future [2]. Solar cell performance on this material class has shown to reach high efficiencies for standard Al-BSF cell technology as well as for "Passivated Emitter and Rear Contact" (PERC) cells [3]. Recently, a champion solar cell with an efficiency of 20.8 % has been demonstrated for a PERC cell structure and advanced cell processes based on a p-type HPM-Si wafer [4, 5].

Analysis of the electronic characteristics of mc-Si wafers with p-type and n-type polarity have pointed out that the minority carrier lifetime in n-type material is less prone to the detrimental influence of some metal impurity species, especially interstitial iron [6] [7]. A high minority carrier lifetime larger than 500 µs could be measured in the middle of grains of passivated n-type mc-Si wafers in the "as-cut" state [8]. However, for material of both polarities structural defects such as dislocation clusters and grain boundaries show high recombination of minority carriers due to decoration with impurities [6].

The combination of the HPM-Si approach and n-type polarity promises a wafer material suitable for high efficiency solar cells. A suitable cell type is the "Tunnel Oxide Passivated Rear Contacts" (TOPCon) cell structure developed at Fraunhofer ISE [9] for n-type bulk wafer material. In contrast to PERC, the full area back contact is connected to the bulk silicon via a stack of layers covering the whole wafer. The current flow in the bulk silicon is predominantly vertical to emitter and back contact. Thus the impact of majority carrier flow across grain boundaries in mc-Si is diminished in comparison to cell concepts with discrete local back contacts. The potential of the TOPCon solar cell concept to realise high efficiency has been demonstrated on Float Zone Si material to be 24.9 % [10]. First cells on n-type HPM-Si with iso-textured front side and single anti-reflection coating have shown very promising results with the best cell reaching an open circuit voltage of 663 mV and a cell efficiency of 19.3 % [11, 12].

This work focuses on the further development of n-type HPM-Si material suitable for solar cells with 20 % efficiency by directional solidification based on seeded growth technology.

2 EXPERIMENTAL PROCEDURE

2.1 Directional solidification process

Two multicrystalline Silicon ingots of research size G1 equivalent to 14 kg silicon and a final height of approximately 120 mm have been produced by directional solidification in a laboratory furnace. Standard industrial type quartz crucibles with a Si_3N_4 release layer applied by spray coating have been used. On the bottom of each crucible, specially adapted seed material was placed up to a height of approx. 30 mm. The rest of the crucible volume was filled with high purity poly-Si feedstock. The resistivity was adjusted by the addition of phosphorus via silicon wafers with high Phosphorus content prior to melting.

The thermal profile applied enforced melting from the top and to some extent from the crucible sides. The bottom of the crucible was kept below 1380 °C for the whole time thus preventing part of the seed material from melting. The thermal profile was kept identical for the two ingots presented in this paper.

2.2 Seed preparation

Crystalline silicon pieces of three different sizes were prepared as seed materials. Undoped granular silicon from a Fluidized Bed Reactor (FBR) process was used as another type of seed material. The size distribution of the beads resembled the standard distribution of the product.

All Si seed pieces except the granular beads were cleaned and etched prior to crystallisation in order not to incorporate any impurities from the preparation process.

In the first ingot, the influence of four different types of seed composition on the crystal quality was investigated. Each quarter of the crucible bottom (Q1-Q4) was filled with a varying composition of crystalline Si pieces:

- Q1 - full mono-Si plate
- Q2 - large sized Si pieces
- Q3 - medium sized Si pieces
- Q4 - small sized Si pieces

In the second ingot, the influence of already crystallised HPM-Si as seed material was investigated. One half of the crucible bottom was covered by a plate, prepared from the upper half of a previously crystallised HPM-Si ingot. The second half of the crucible bottom was filled with granular material.

2.3 Material processing

After crystallisation two opposite side faces of each ingot were symmetrically cut off. The cross sections of approx. 200 mm width and 120 mm height were mechanically polished as prerequisite for further analysis. The bottom part with 30 mm height and the top part above 110 mm ingot height were cut off each ingot. 180 µm thick wafers with side length of 156 mm were prepared from the centre material and analysed for crystal structure characteristics.

Selected wafer stacks from medium and top region of the ingots were reduced to 125 mm side length by laser cutting due to further processing reasons. For both height positions, one wafer received a boron diffusion at 890 °C for 1h as used for the TOPCon cell process. The indiffused layer was subsequently etched off again. All wafers for lifetime analysis received a silicon nitride layer at both sides as surface passivation layers.

2.4 Material analysis

The resistivity distribution in each ingot was measured by eddy current mappings at the polished cross sections.

The fraction of wafer area affected by dislocation clusters was calculated by automated analysis of photoluminescence images taken from all wafers directly after wafer cutting. The grain structure of each wafer was optically identified on the wafer surfaces [13]. The mean grain area was determined via image analysis. All quantities were calculated with respect to the wafer area corresponding to one type of seed composition.

The material quality was investigated by photoluminescence imaging (PLI) at low injection conditions calibrated by harmonically modulated photoluminescence [14] in order to obtain images of the minority carrier lifetime. A mean lifetime τ_{mean} was calculated via the harmonic mean of the square root of the spatially resolved lifetime values $\tau(x,y)$.

A prediction of the solar cell efficiency potential was made by an "Efficiency limiting bulk recombination analysis" (ELBA) [15] (with the modifications described in [16]). Efficiency maps were calculated by combining injection-dependent images of bulk recombination with PC1D cell simulations of the TOPCon cell structure applied in the aforementioned work [12]. The calculated average efficiencies refer to the wafer areas corresponding to the different seeding compositions.

3 RESULTS

3.1 Resistivity distribution

A resistivity range between 2.2 Ωcm near the remaining seed material and 0.4 Ωcm near the ingot top was reached for all ingots. Figure 1 shows the spatial distribution for the second ingot.

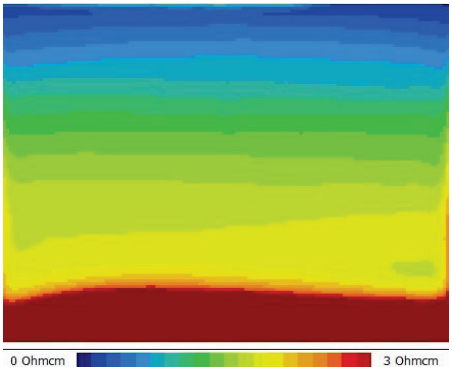

Figure 1: Resistivity distribution at cross section of ingot 2 measured by eddy current method.

The remaining seed material visible as red region with significant higher resistivity exhibits a convex form. Since iso-lines of the resistivity resemble the solid-liquid interface during crystal growth, it is apparent that an interface shape from flat to slightly convex with respect to the solid could be maintained up to the ingot top for the applied thermal recipe.

3.2 Grain size development

For each seed composition, the height dependent average grain size has been evaluated on wafer level with respect to the corresponding wafer areas (see Figure 2). The following evaluation focuses on material grown on medium, small and granular seeds as well as the seed plate.

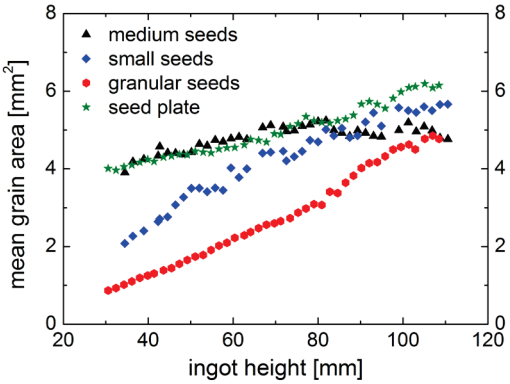

Figure 2: Mean grain size for different seed compositions evaluated on wafer level.

For all seed types an increase of grain size can be observed. The rate of increase over height shows a tendency with higher rates for smaller sized initial grains thus diminishing the difference in mean size between the materials over height. The curves for the medium seeds and the seed plate show the same behaviour until a height of approx. 80 mm with a further flattening of the profile for the medium sized seeds.

3.3 Dislocated area fraction

The height profiles showing the area fraction affected by dislocation clusters exhibit a similar general trend (see Figure 3). The material on small seeds has significantly less dislocated wafer area than the one on medium sized seeds up to a height of approx. 90 mm. For the ingot top, both curves coincide.

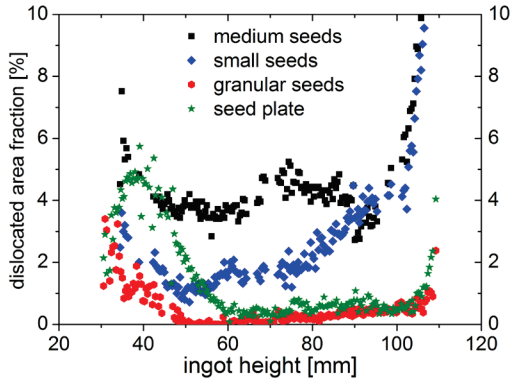

Figure 3: Height profiles of the area fraction affected by dislocation clusters, measured in the as cut state.

The lowest dislocated area is found for the material grown from granular seeds which already showed the smallest initial grain sizes. After a decrease from 4 % on the first wafer at 30 mm to almost the detection limit at 50 mm, the profile is very flat and below 1 % until a sharp rise at 107 mm near the ingot top.

The profile for the seed plate shows a deviating behaviour. After initially having up to 5 % covered by dislocation clusters, a reduction of dislocation clusters can be observed to a level almost as low as for the granular seed material. Interestingly, a sharp rise at the ingot top occurs for both profiles in the same manner, but differing from the rise for the other two profiles.

3.4 Lifetime distribution

The lifetime distribution on wafer level for all seeding types was evaluated by PLI images on passivated wafers for the "as cut" state and after Boron diffusion as the characteristic high temperature step. The PL images reveal a lifetime distribution for a specific injection of 0.05 suns.

Figure 4 shows the mean lifetime for "as cut" wafers from all considered seed compositions at a medium height position of 66 mm and a top region of 96 mm, respectively.

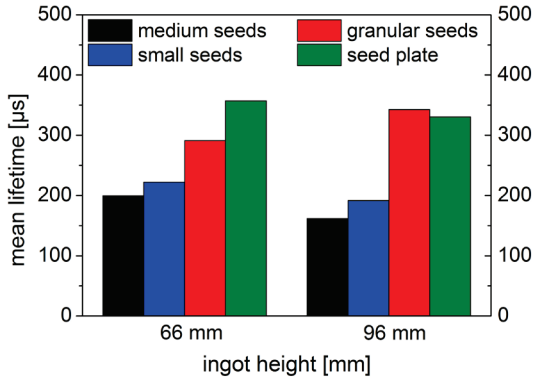

Figure 4: Mean lifetime in "as-cut state" for medium and top regions.

The wafers in the medium ingot region reveal a clear dependence on the seed composition, with increasing values for decreasing initial grain sizes at the areas with Si pieces and granular material as seed. The mean lifetime for the medium seed wafer shows the lowest value of 200 µs. Although the mean initial grain size in the seed plate is very similar to the size for the medium seed material, the seed plate material shows the highest mean lifetime in the middle region of 357 µs and thus 157 µs higher than the medium seed material. The values for the medium and small seed material as well as for the seed plate decrease for the top region whereas it increases for the granular seed material.

The wafers after Boron diffusion show an opposite trend for the middle region at 66 mm ingot height (see Figure 5). The mean lifetime of the medium seed material increases in comparison to the "as-cut state" whereas the lifetime for the granular seed material decreases.

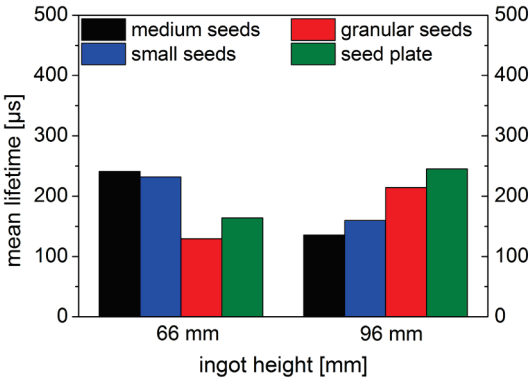

Figure 5: Mean lifetime after Boron diffusion for medium and top regions.

The trend for the top region at 96 mm ingot height is similar to the "as-cut state", but on a significantly lower level.

3.5 Efficiency prediction by ELBA

The ELBA procedure evaluated injection-dependent lifetime images of the previously described wafers. In addition to lifetime information, other electronic properties such as resistivity and local carrier densities are considered for the prediction of solar cell efficiency.

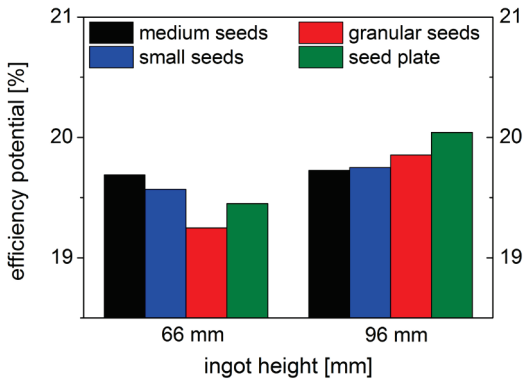

Figure 6: Cell efficiency potential predicted by ELBA for medium and top region.

The predicted cell efficiencies for both ingot heights show the same tendency as the lifetime analysis after

Boron diffusion (see Figure 6). In the top region, the relative difference between the materials diminishes in comparison to the lifetime values. Furthermore, the efficiency values of the materials in the top region are on higher level as the ones for the medium height, which is significantly different from the situation for the lifetime values.

The predicted efficiency of a TOPCon cell on seed plate material of the top region is 20.0 % with the assumption of an iso-textured front side, single anti-reflection coating and no further high temperature processing steps such as e.g. additional Phosphorous gettering.

4 DISCUSSION

The results of the lifetime analysis for the "as-cut state" and the state after Boron diffusion reveal that for the investigated materials both mean grain size and dislocated area fraction can be limiting parameters.

Carrier recombination takes place both at dislocation clusters and grain boundaries as recombination active structural defects. The calculated mean grain size is in principle inversely proportional to the added length of all grain boundaries and thus represents total recombination at grain boundaries. Within the scope of this paper, the recombination activity of different types of dislocations or grain boundaries has not been investigated.

In the "as-cut state" a general correlation between mean lifetime values and dislocated area fractions is found. In contrast, an inverse correlation is found for mean lifetime and mean grain size.

The lifetime value of the medium seed material for 66 mm height is significantly lower than for the seed plate material at the same height. Although both materials have the same mean grain size, the dislocated area fraction of the medium seed material is significantly higher. This would fit to a lifetime limitation by recombination at dislocation clusters. The granular seed material has a similar dislocated area fraction, but a significantly lower mean grain size than the seed plate material. Therefore, the lifetime in the "as-cut state" is grain boundary limited and thus lower for the material from granular seeds.

The boron diffusion has a positive gettering effect on dissolved impurities. The concentration of impurities within the grains can be reduced. However, the high temperature during the diffusion process can trigger a release of agglomerated impurities at dislocations and grain boundaries. Therefore, the net effect of boron diffusion on the mean lifetime is strongly depending on the proportion of structural defects to grain volume. This is most likely the reason for the differing trend in the mean lifetime after boron diffusion at medium ingot height with the medium seed material giving the highest values in contrast to the "as-cut state". The development of mean lifetime for the other materials is in accordance with this mechanism.

Thus, the analysis of mean grain size and dislocated area fraction can explain the observed lifetime characteristics. However, the comparison of the lifetime values after boron diffusion with the predicted cell efficiencies after ELBA simulation shows, that an analysis of just the two parameters mean grain size and dislocated area fraction is not enough to deduce the ratio between these materials on efficiency level. The increased efficiency level of the studied materials in the top region in comparison to the medium height region cannot be explained just by an assessment of these two parameters. Further parameters such as e.g. net resistivity and injection dependence of predominant defects have to be taken into account as well. On efficiency level, material from the top region benefits from a higher base doping concentration compared with lower ingot heights.

The investigated material grown from an HPM-Si plate seems to be a good compromise between large grains and low dislocated area fraction in order to achieve high cell efficiencies for wafers from all ingot heights. The best wafer of this type shows an expected efficiency value of 20 %. By further optimization of grain size and orientation in conjunction with low fraction of dislocated areas and generally reduced impurity levels, higher cell efficiencies seem to be possible for the investigated cell structure. Especially in combination with the application of an advanced texturing as, e.g. high quality plasma texture, cell efficiencies of 21-22 % seem to be feasible on HPM-Si substrate [12].

5 CONCLUSIONS

The efficiency potential of HPM-Si strongly depends on both initial grain size and crystal structure as initiated by the applied seeding material. The investigation of different seeding compositions has shown that both grain size and dislocated area fraction can limit the lifetime after boron diffusion and thus the achievable cell efficiency of the investigated TOPCon cells. For the use of a plate of HPM-Si material as seed as a compromise between grain size and dislocated area fraction, an efficiency of 20 % is predicted by an ELBA analysis.

By further optimization of n-type HPM-Si material and cell processing, efficiencies exceeding 21 % for advanced cell concepts such as TOPCon are expected.

6 ACKNOWLEDGMENTS

The authors would like to thank Wacker Polysilicon for the silicon materials and express their gratitude to the crystallisation, cell processing and characterization teams at ISE for their support and input in many valuable discussions. This work was funded by the German Federal Ministry for the Economy and Energy (THESSO project FKZ 0325491).

7 REFERENCES

[1] Y. M. Yang, A. Yu, B. Hsu, W. C. Hsu, A. Yang, and C. W. Lan, "Development of high-performance multicrystalline silicon for photovoltaic industry," *Progress in Photovoltaics: Research and Applications,* vol. 23, pp. 340-351, 2015.

[2] A. Metz et al., "International Technology Roadmap for Photovoltaic Results 2014" Rev.1, July 2015, http://www.itrpv.net/

[3] S. Engelhart et al., "3 Years of High Quality mc-Si PERC Production Experience," in *Proceedings of the 31th European Photovoltaic Solar Energy Conference*, Hamburg, Germany, 2015, in print.

[4] P. Verlinden, W. Deng, X. Zhang, Y. Yang, J. Xu, Y. Shu, P. Quan, J. Sheng, S. Zhang, J. Bao, F. Ping, Y. Zhang, and Z. Feng, "Strategy, Development and Mass Production of High-Efficiency Crystalline Si PV Modules," presented at the 6th World Conference on PV Energy Conversion, Kyoto, Japan, 2014.

[5] M. A. Green, K. Emery, Y. Hishikawa, W. Warta, and E. D. Dunlop, "Solar cell efficiency tables (Version 45)," *Progress in Photovoltaics: Research and Applications,* vol. 23, pp. 1-9, 2015.

[6] F. Schindler, B. Michl, A. Kleiber, H. Steinkemper, J. Schon, W. Kwapil, P. Krenckel, S. Riepe, W. Warta, and M. C. Schubert, "Potential Gain in Multicrystalline Silicon Solar Cell Efficiency by n-Type Doping," *IEEE Journal of Photovoltaics,* vol. 5, pp. 499-506, 2015.

[7] D. Macdonald and L. J. Geerligs, "Recombination activity of interstitial iron and other transition metal point defects in p- and n-type crystalline silicon," *Applied Physics Letters,* vol. 85, pp. 4061-3, 2004.

[8] J. Schön, F. Schindler, W. Kwapil, M. Knörlein, P. Krenckel, S. Riepe, W. Warta, and M. C. Schubert, "Identification of the most relevant metal impurities in mc n-type silicon for solar cells," *Solar Energy Materials and Solar Cells,* vol. 142, pp. 107-115, 2015.

[9] F. Feldmann, M. Bivour, C. Reichel, H. Steinkemper, M. Hermle, and S. W. Glunz, "Tunnel oxide passivated contacts as an alternative to partial rear contacts," *Solar Energy Materials and Solar Cells,* vol. 131, pp. 46-50, 2014.

[10] M. Hermle, F. Feldmann, J. Eisenlohr, J. Benick, A. Richter, B. Lee, P. Stradins, A. Rohatgi, and S. W. Glunz, "Approaching Efficiencies above 25% with both Sides-contacted Silicon Solar Cells," *IEEE Journal of Photovoltaics,* submitted for publication, 2015.

[11] F. Schindler, B. Michl, P. Krenckel, S. Riepe, F. Feldmann, J. Benick, W. Warta, and M. C. Schubert, "Efficiency Potential of p- and n-type High Performance Multicrystalline Silicon," *Energy Procedia,* vol. 77, pp. 633-638, 2015.

[12] F. Schindler, J. Schön, B. Michl, S. Riepe, P. Krenckel, J. Benick, F. Feldmann, M. Hermle, S. W. Glunz, W. Warta, and M. C. Schubert, "High Efficiency Multicrystalline Silicon Solar Cells: Potential of n-type Doping," *IEEE Journal of Photovoltaics,* accepted for publication, 2015.

[13] http://www.intego.de/en/new-product-grain-size

[14] J. A. Giesecke, M. C. Schubert, B. Michl, F. Schindler, and W. Warta, "Minority carrier lifetime imaging of silicon wafers calibrated by quasi-steady-state photoluminescence," *Solar Energy Materials and Solar Cells,* vol. 95, pp. 1011-1018, 2011.

[15] B. Michl, M. Rüdiger, J. Giesecke, M. Hermle, W. Warta, and M. C. Schubert, "Efficiency limiting bulk recombination in multicrystalline silicon solar cells," *Solar Energy Materials & Solar Cells,* vol. 98, pp. 441-447, 2012.

[16] B. Michl, M. Kasemann, W. Warta, and M. C. Schubert, "Wafer thickness optimization for silicon solar cells of heterogeneous material quality," *Physica Status Solidi RRL – Rapid Research Letters,* vol. 7, pp. 955-958, 2013.